Time Domain Model Validation Results

Introduction

In order to analyze the behavior of various wave-energy extraction devices, a general purpose numerical model has been developed that can be configured to model different design concepts. Because this model makes a number of simplifying assumptions, it's important to validate the results of a typical system against experimental results. This report outlines and compares the numerical and experimental results for a simple case of a floating buoy that supports a submerged heavy body 20 meters below the buoy. The two bodies are connected by a hydraulic ram system that behaves like a damped spring element. To validate the model, this system was deployed in Monterey Bay on August 10th and 11th, 2009. The sea state during the tests and the resulting motions of the system were measured and recorded. Subsequent to this experiment the numerical model was run using the sea state from the test days as an input and the results were compared. In addition to the at-sea testing, a step response test of the system was performed in the MBARI test-tank, which consisted of dropping the buoy from a small elevation and measuring the resulting tension and elongation step response.

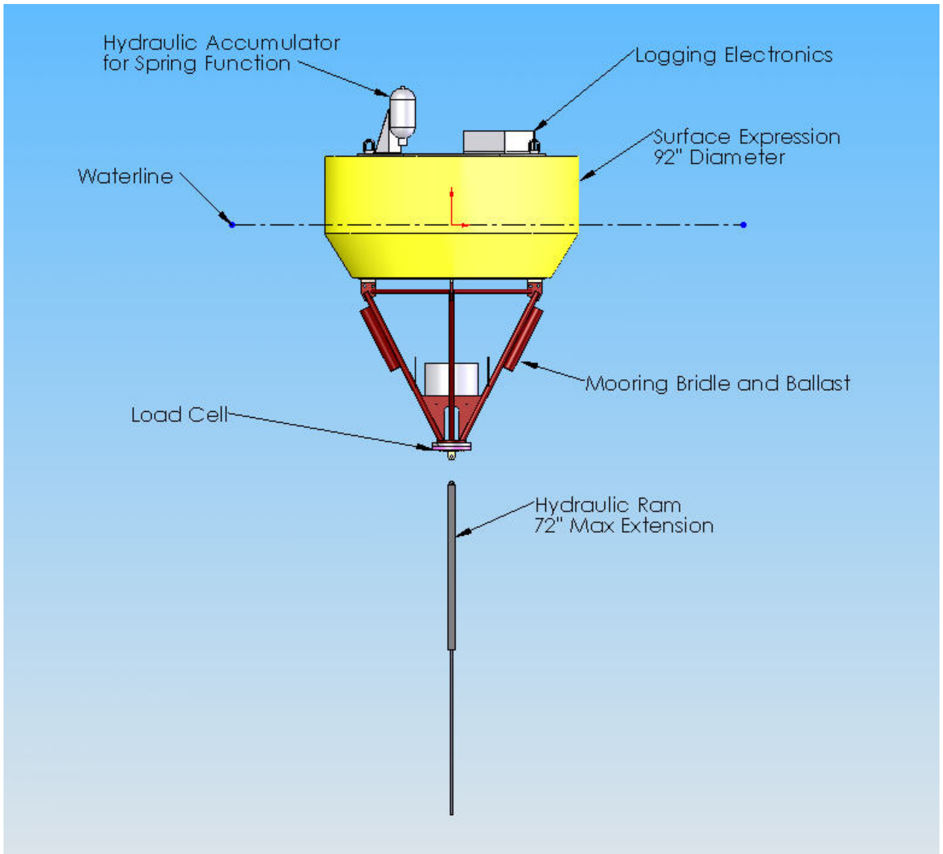

Figure 1: Surface expression and hydraulic cylinder acting as spring/damper system. Flat plate or sphere is connected and submerged at a depth of 20 meters.

Experimental Set-Up

The experimental set-up consists of a cylindrical surface float and a submerged element that is connected by a hydraulic ram system that behaves as a spring element. Figure 1 shows the surface-buoy configuration. Two different submerged elements were used, a 48" diameter flat plate and a 28" diameter sphere. These two elements were used to provide some variation in the device configuration; the numerical model was run in both configurations as well. The details of the two configurations that were tested are outlined below:

Configuration I

Floating Body: MOOS Buoy

- Total Mass: 2600 lbs (1179.34 kg)
  (includes Hydraulic ram, Instruments, Accumulators, Heave Sensor and Bridle assembly)
- Waterline: 4 inches (0.1016 m) above Chine (Location of Origin)
- Center of Gravity: [0, 0, -0.63m]
- Center of Buoyancy: [0, 0, -0.26m]
- Displacement: 1.64 m^3
- Moment of Inertia about Origin
  I_{xx} = 1998.19 kg m^2
  I_{yy} = 1947.66 kg m^2
  I_{zz} = 466.13 kg m^2
- Tether Point of Attachment: 2.0 m below chine (2.09 m below waterline)
- Tether Length = 3.0m (test-tank tests), 20.0m (at-sea tests)

Submerged Body: Flat Circular Plate

- Total Mass: 1297 lbs (588.31 kg)
- Radius: 2 ft (0.6096 m)
- Thickness: 2.5 inches (0.0635m)
- Displacement: 0.074133 m^3
- Center of Gravity: [0, 0, 0]
- Center of Buoyancy: [0, 0, 0]
- Moment of Inertia about Origin
  I_{xx} = 55.22 kg.m^2
  I_{yy} = 55.26 kg.m^2
  I_{zz} = 110.08 kg.m^2
- Tether Point of Attachment = (54.25 inches) 1.37795 m above CG of plate

Configuration II

Floating Body: MOOS Buoy

- Total Mass: 2600 lbs (1179.34 kg)
  (includes Hydraulic ram, Instruments, Accumulators, Heave Sensor and Bridle assembly)
- Waterline: 2.25 inches (5.715 cm) above Chine
- Center of Gravity: [0, 0, -0.63m]
- Center of Buoyancy: [0, 0, -0.29 m]
- Displacement: 1.475 m^3

- Moment of Inertia about Origin
  I_{xx} = 1998.19 kg.m ^{2}
  I_{yy} = 1947.66 kg.m ^{2}
  I_{zz} = 466.13 kg.m ^{2}
- Tether Point of Attachment: 2.0 m below chine (2.09 m below waterline)
- Length of tether: 20m (at-sea tests)

<u>Submerged Body No. 2: Solid Sphere</u>

- Total Mass: 1175 lbs (532.97 kg)
- Radius: 14 inches (0.3556 m)
- Displacement: 0.0188354 m ^{3}
- Center of Gravity: [0, 0, 0]
- Center of Buoyancy: [0, 0, 0]
- Moment of Inertia about Origin
  I_{xx} = 26.958 kg.m ^{2}
  I_{yy} = 26.958 kg.m ^{2}
  I_{zz} = 26.958 kg.m ^{2}
- Tether Point of Attachment = (14 inches) 0.3556 m above CG of sphere.

Hydraulic System Description

The spring/damper system is constructed from industrial hydraulic components, a 72" long linear ram provides compliance and is plumbed to a system of accumulators and valves that provides a spring effect (force proportional to displacement) and a damping effect (force proportional to velocity). Because it is difficult to construct a perfectly linear spring and damper system from these hydraulic components, the actual characteristics of the spring/damper system was measured for inclusion in the numerical model. Figure 2 depicts a schematic representation of the hydraulic system designed and used in the validation experiment. Three accumulators of capacities 1 quart, half gallon and one gallon with precharges 50, 200, 500 psi respectively, provide the required spring force. A pressure sensor (P1) was connected to measure the pressure in the system which is proportional to the tension in the tether.

The spring force in the system is a result of the gas being compressed in the accumulators as the piston rod extends, this is not a linear phenomenon but the three accumulators in parallel approximate a linear spring as shown in the measured force versus elongation results (Figure 3). This measured spring relationship is what is used in the numerical model.

The measured damping force present in the experimental set-up is shown in figure 4, this highly nonlinear damping relationship is approximated for purposes of inclusion in the model in terms of elongation rate 'v' as

$$Fd = \frac{\Delta F}{2}\left(1 - \exp(-\alpha v)\right) sign(v) \tag{3}$$

where

ΔF = mean damping force in N/(m/s)

α = velocity slope coefficient (1/(m/s))

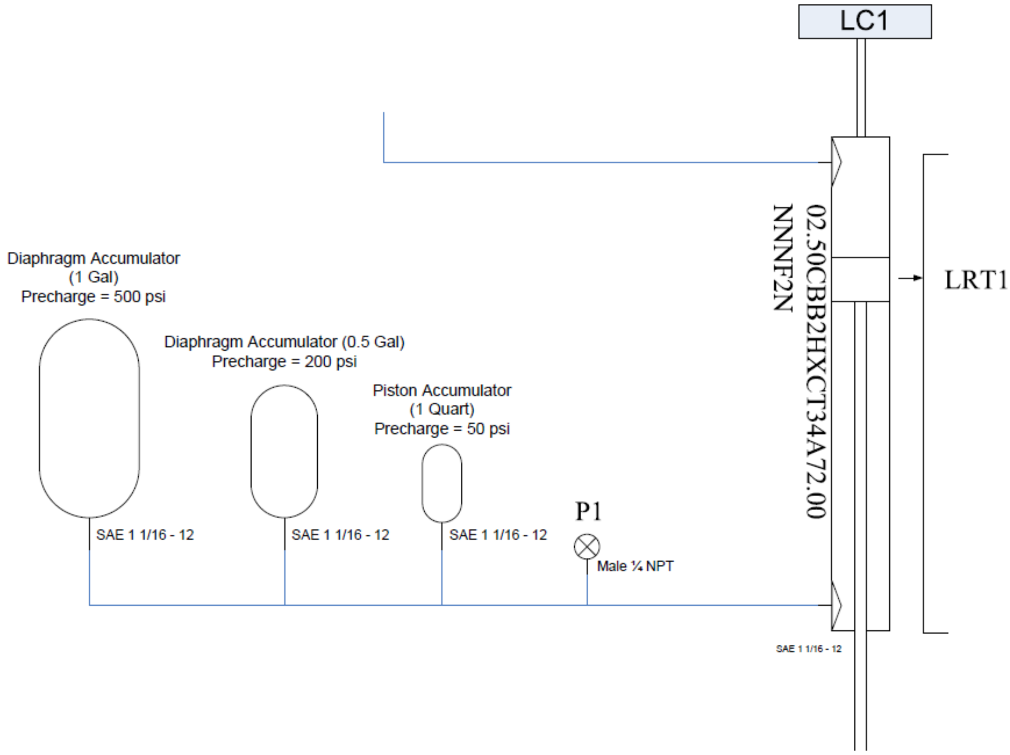

Figure 2. Schematic drawing of the hydraulic components showing the ram, the accumulator system, load cell (LC1), pressure sensor (P1) and potentiometer (LRT1).

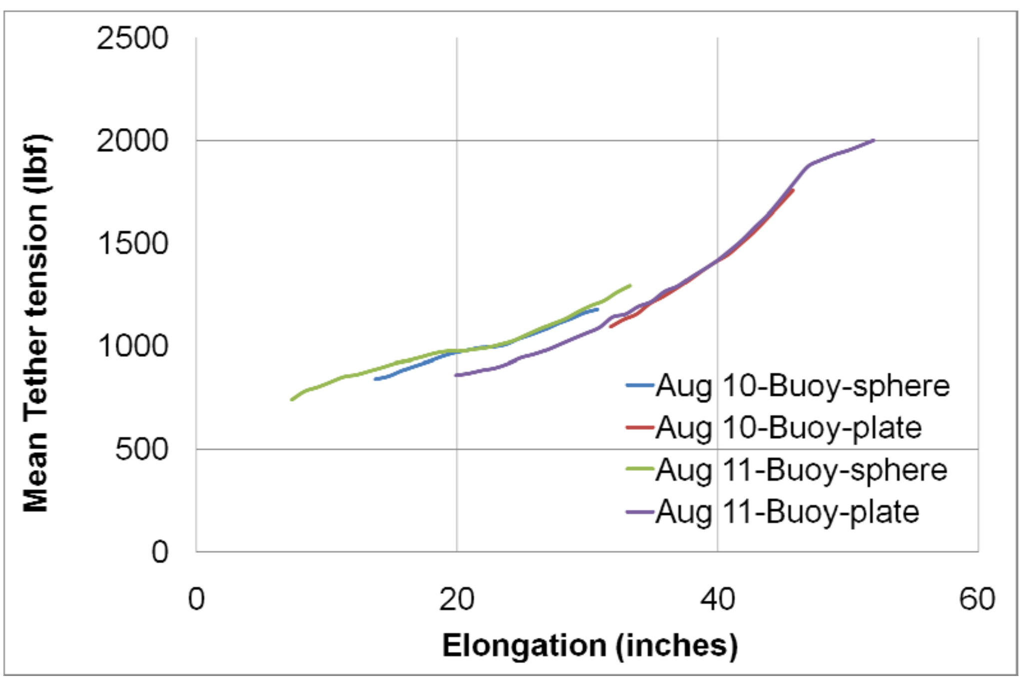

Figure 3. Experimental measurements of mean tether tension as a function of tether elongation.

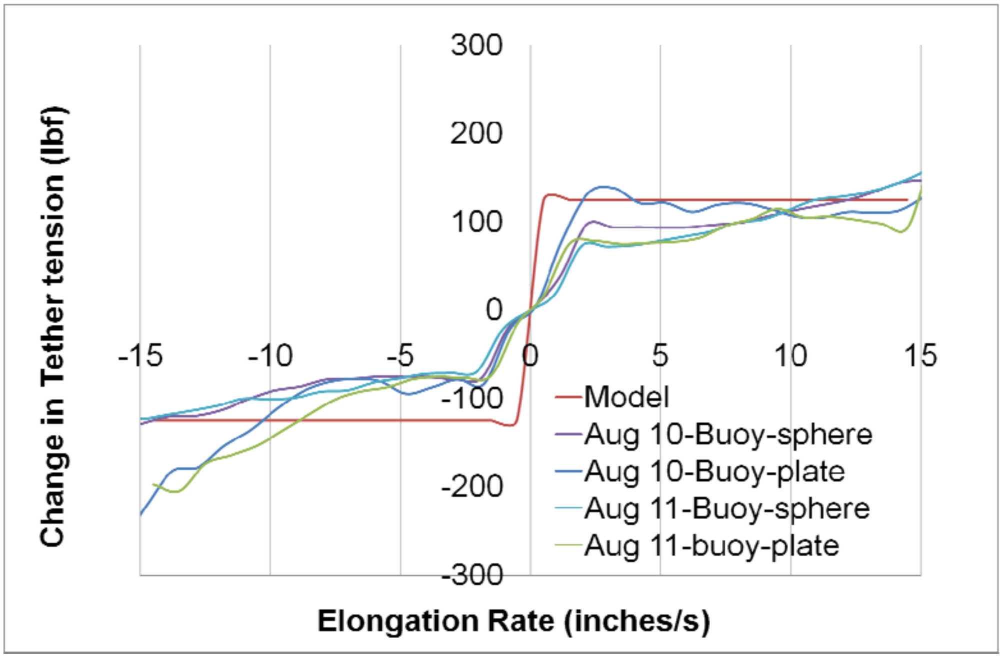

Figure 4. Variation of tether tension about the mean value in Figure 3 measured at variable tether elongation rates.

To measure the actual tensions in the system, a load cell was bolted to the lower end of the bridle to measure the tension force acting on the tether connecting the submerged element to the surface float (see figure 1). The stroke of the hydraulic ram and the resulting tether elongation was measured by a built-in potentiometer in the hydraulic ram.

The incoming wave field was measured by a nearby wave-measurement buoy. A significant wave height of 1.0 m at a peak period of 7.2 seconds were recorded on August 10th near the experimental site whereas the wave conditions were considerably milder on August 11th with the significant wave height and peak period values being 0.7 m and 8 seconds respectively. The wave spectral plots appear in figures 7 to 10. Field experimental results are sub-divided into four datasets for the ease of understanding, namely, Buoy-plate August 10th, Buoy-plate August 11th, Buoy-sphere August 10th and Buoy-sphere August 11th.

All quantities of tension, pressure and elongation were logged on-board the buoy at 100Hz for later analysis.

Additional Calibration Information

Figure 5 shows the calibration chart of the potentiometer built into the hydraulic ram used to measure the elongation of the tether connecting the surface buoy to the submerged element. Voltage changes nearly linearly with elongation. An extension of approximately 15 inches changes the measured voltage by 1 volt.

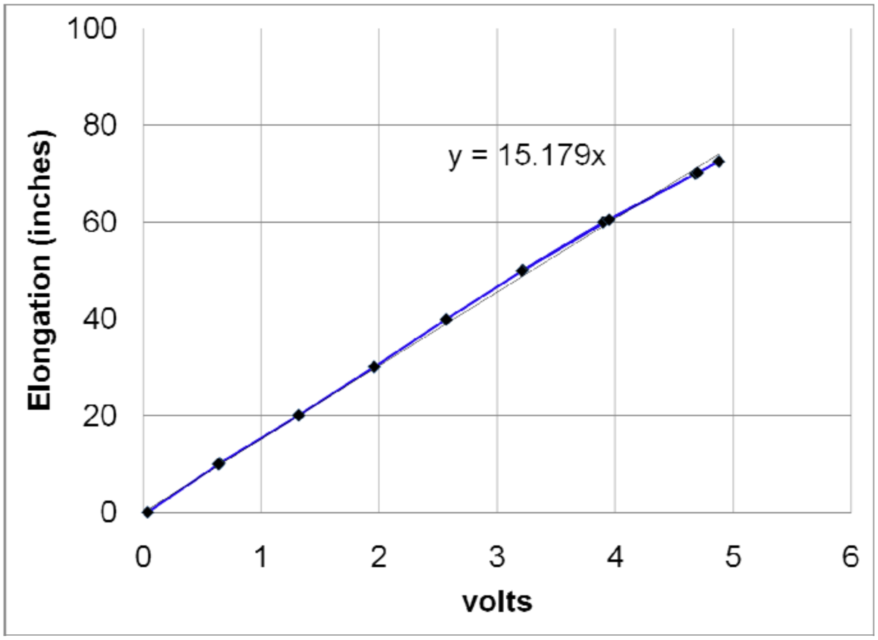

Figure 5. Experimental measurement of potentiometer calibration

Numerical Model

The numerical model consists of an equation of motion solver that computes the resulting motion in three dimensions of a collection of floating and submerged bodies that are subject to external forcing acting on the various bodies that make up the system. The forces acting on the surface buoy include weight, hydrostatic force, wave-exciting force, wave radiation force, skin-friction and pressure drag and the tether tension. The submerged element (sphere/plate) is forced by weight, hydrostatic force, skin-friction and pressure drag and the tether tension. The hydrodynamic frequency-domain coefficients were calculated by using WAMIT Version 6.4. WAMIT is a radiation/diffraction code developed for the analysis of the interaction of surface waves with floating bodies. A separate utility was used to evaluate time-domain impulse response functions from the outputs of WAMIT.

Results and Discussion

Two types of tests were performed for the purpose of validating the numerical model. A step response test was conducted in the MBARI test tank and two days of testing was performed at sea to measure the systems response to ocean waves.

Step Response test

The step response experiment was conducted in the MBARI test tank on the Buoy-plate system, the buoy was lifted to a height of 12 inches and released. Experimental and modeling results of the step response test are presented in figure 6. There is excellent agreement in the phase of the motion response and tether elongation but the magnitude of tether tension is underestimated in the modeled results. This discrepancy is most likely due to the fact that the elongation rates are very high step response tests and the modeled results fails to accurately simulate the damping forces in the ram at a very high rate of tether elongation. The tension results show a high frequency disturbance at the two and four second marks. Based on observation of video of the tests, this interaction appears to be the effect of waves reflecting from the walls of the test tank.

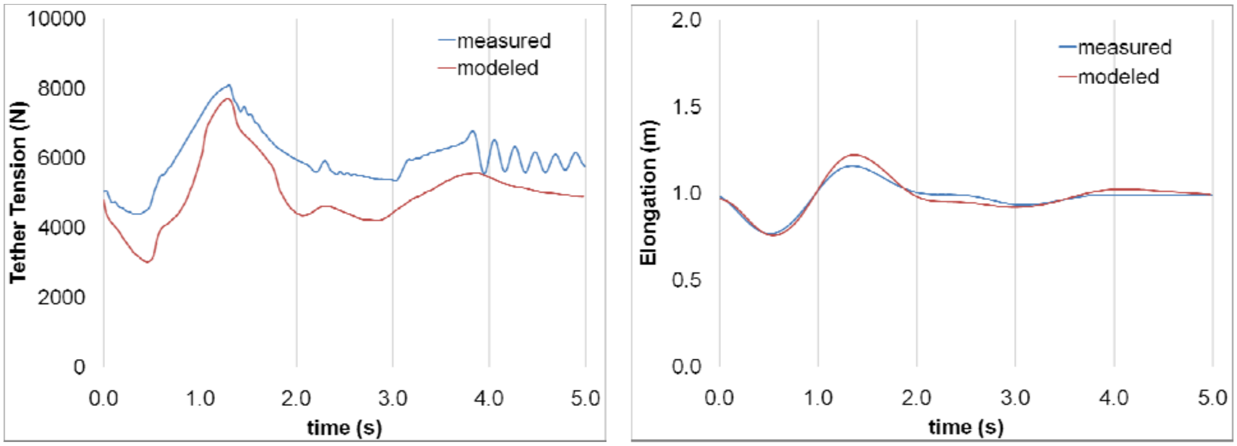

Figure 6. Experimental measurements and model generated values of tether tension and elongation during the step response test.

Monterey Bay Field experiment

Experimental measurements and modeling results of the systems tension and elongation response are plotted in figures 7 to 10 along with concurrent measurements of wave time history and spectra. Comparisons were made for the purposes of validating the numerical modeling results against the experimental observations of tether tension. To accurately model the hydraulic ram dynamics, the experimental observations of spring and damping force as a function of elongation and elongation rate respectively were incorporated into the model. Laboratory experiments were also conducted for confirming the spring and damping forces observed in the field experiments. At small elongation rates, the hydraulic ram dynamics was well understood. At rates exceeding 10 inches/s, there was some amount of uncertainty in the dynamic behavior of the hydraulic ram.

Comparison of experimental observations with numerical modeling results indicates reasonably good agreement. The simplified numerical model captures the buoy-plate and the buoy-sphere system hydrodynamics fairly well as illustrated in figures 7 to 10. In all cases the elongation and tension spectra have a pronounced peak at a frequency that is higher than the peak of the incoming wave spectra, this appears to be related to the natural frequency of the tether system.

The motion of the submerged body attached to the hydraulic ram can be analyzed as a single degree of freedom system oscillating along the heave direction. In this case the natural frequency of the hydraulic cylinder motion is given by

$$f_n = \frac{1}{2\pi}\sqrt{\frac{k}{m+a}} \tag{1}$$

where f_n = natural frequency in Hertz
k = Spring stiffness (N/m)
m = mass of the submerged object (kg)
a = added mass of the submerged object (kg)

Table 1 shows the expected natural frequency of the two configurations based upon linearized estimates of spring stiffness based upon the measured values of force versus elongation shown in figure 3.

Submerged Body	*k (N/m)*	*m (kg)*	*a (kg)*	*Tn (s)*	*fn (Hz)*
Circular Plate	4879.6	588.3	632.2	3.14	0.32
Sphere	2065.0	533.0	193.1	3.73	0.27

Table 1. Linearized hydraulic ram oscillation characteristics.

Results show that a near-zero frequency response exists when the wave exciting force is not high enough to overcome the frictional force which causes the ram to get stuck at one particular location for several seconds. For a buoy-sphere system, the variation of tether tension due to the oscillatory wave motion is about half of that of the buoy-plate system. Lower tension variation causes several instances of mechanical stiction to occur. On the other hand, tether elongation measurements for the buoy-plate system show very little stiction. The numerical model is not able to replicate the stiction mechanism observed in experiments and therefore, the near-zero frequency response is absent in the modeling results. Instead, it is represented as a low amplitude time variation in the plot of elongation with time.

The hydrodynamic damping force acting on the sphere is much lower in magnitude as compared to that of a flat plate. As a result, it takes considerably longer for the sphere to come to rest at the equilibrium position. The rate of tether elongation remains linear for small variations in tether tension and tends to become constant at higher values. Due to low damping, it does not become non-linear. For the system with a flat plate as the submerged element, high damping values tend to introduce non-linearity for large variations in tether tension. The non-linear frequency response is observed in experimental measurements at frequencies higher than the wave excitation frequencies.

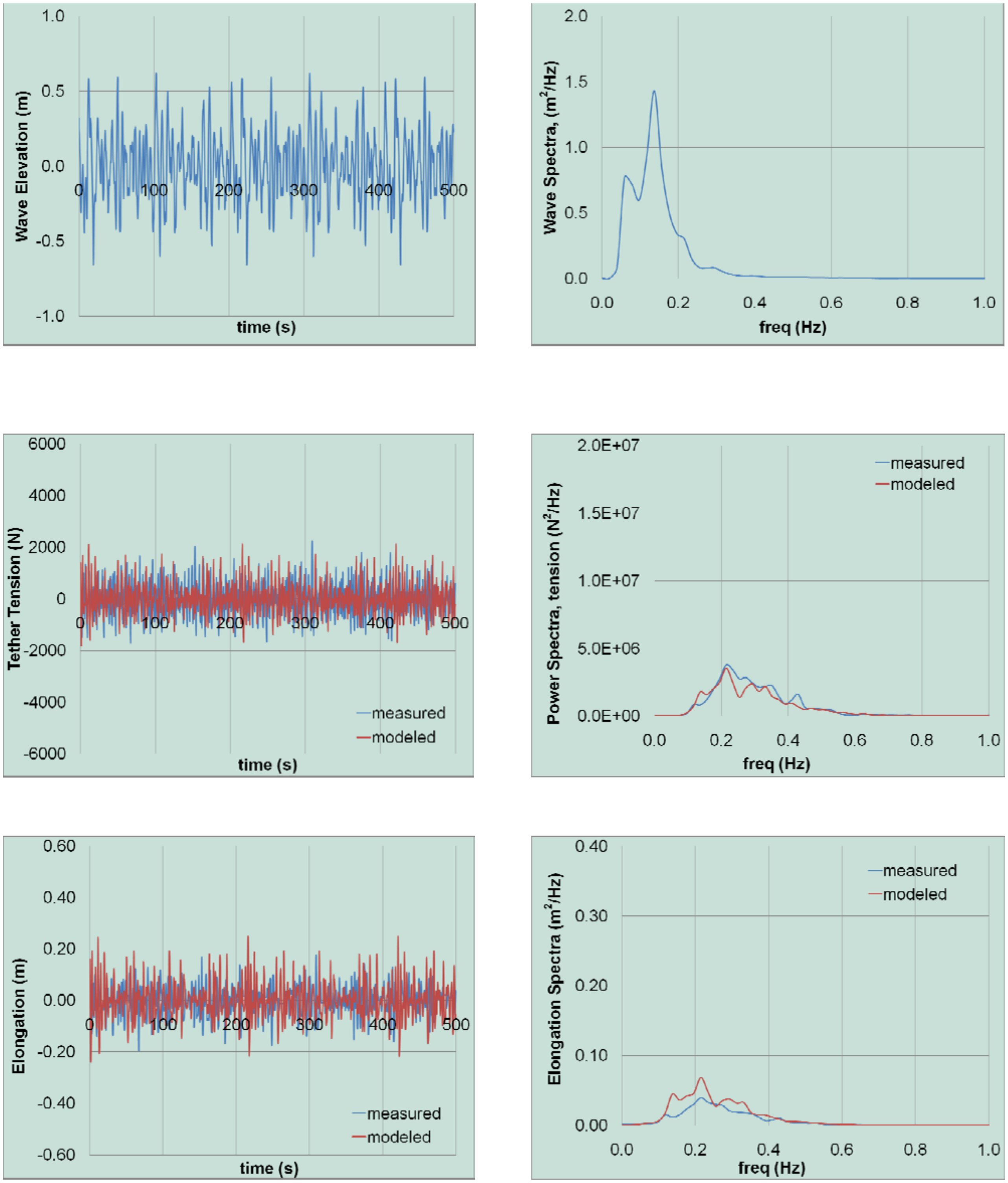

Figure 7. Time history and corresponding spectra of wave elevation, measured and modeled tether tension and elongation. (Buoy-plate Aug 11, 2009)

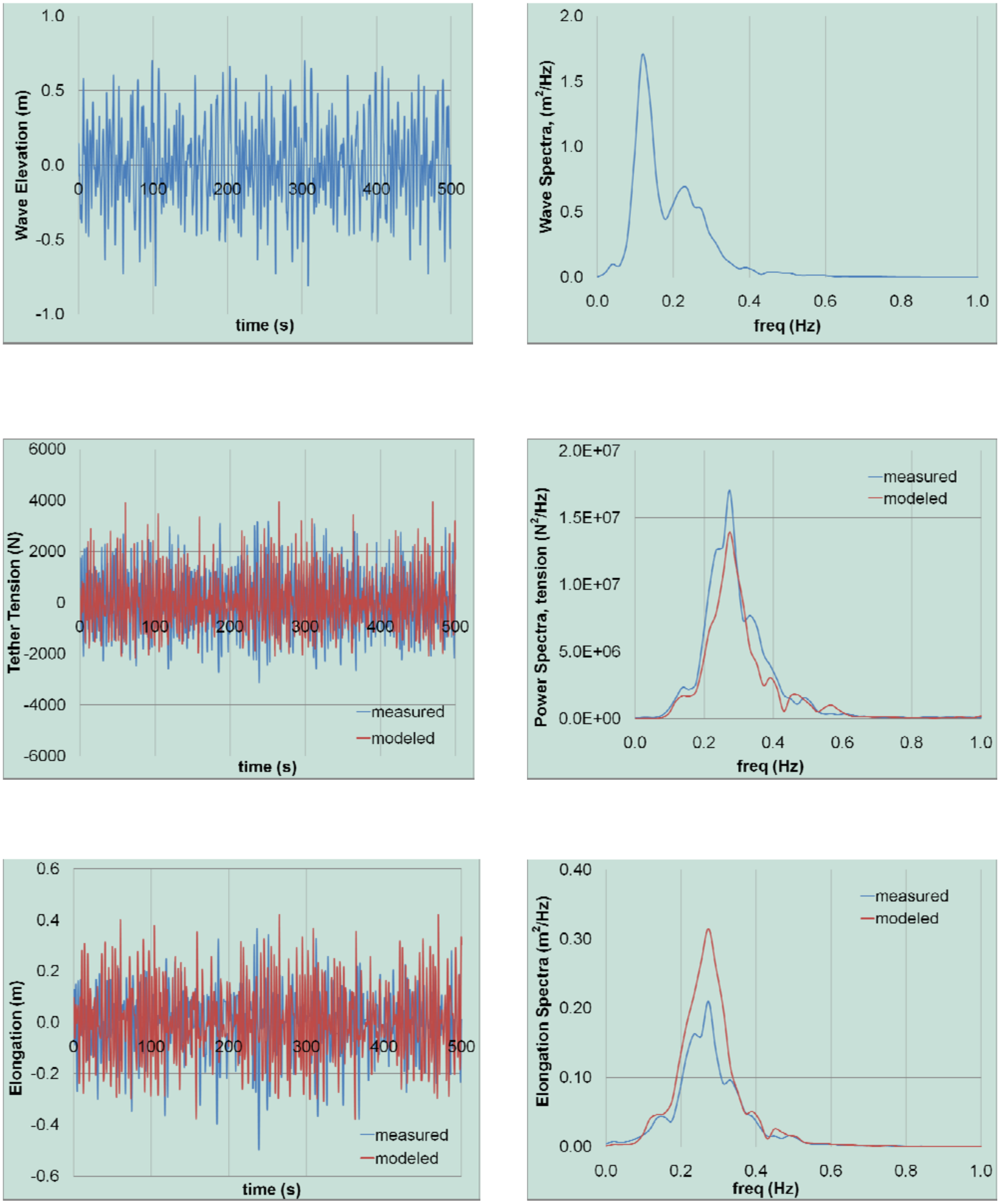

Figure 8. Time history and corresponding spectra of wave elevation, measured and modeled tether tension and elongation. (Buoy-plate Aug 10, 2009)

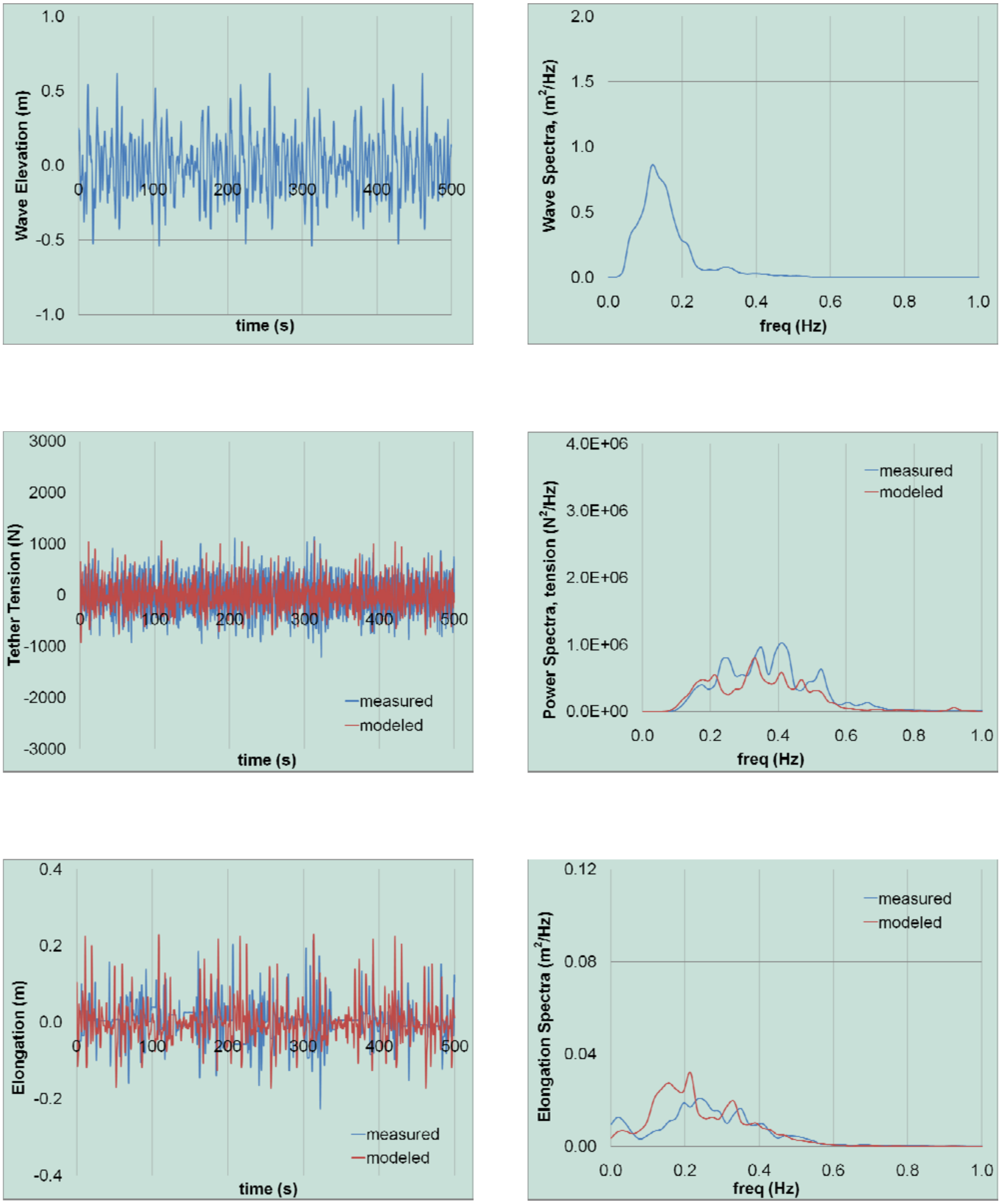

Figure 9. Time history and corresponding spectra of wave elevation, measured and modeled tether tension and elongation. (Buoy-sphere Aug 11, 2009)

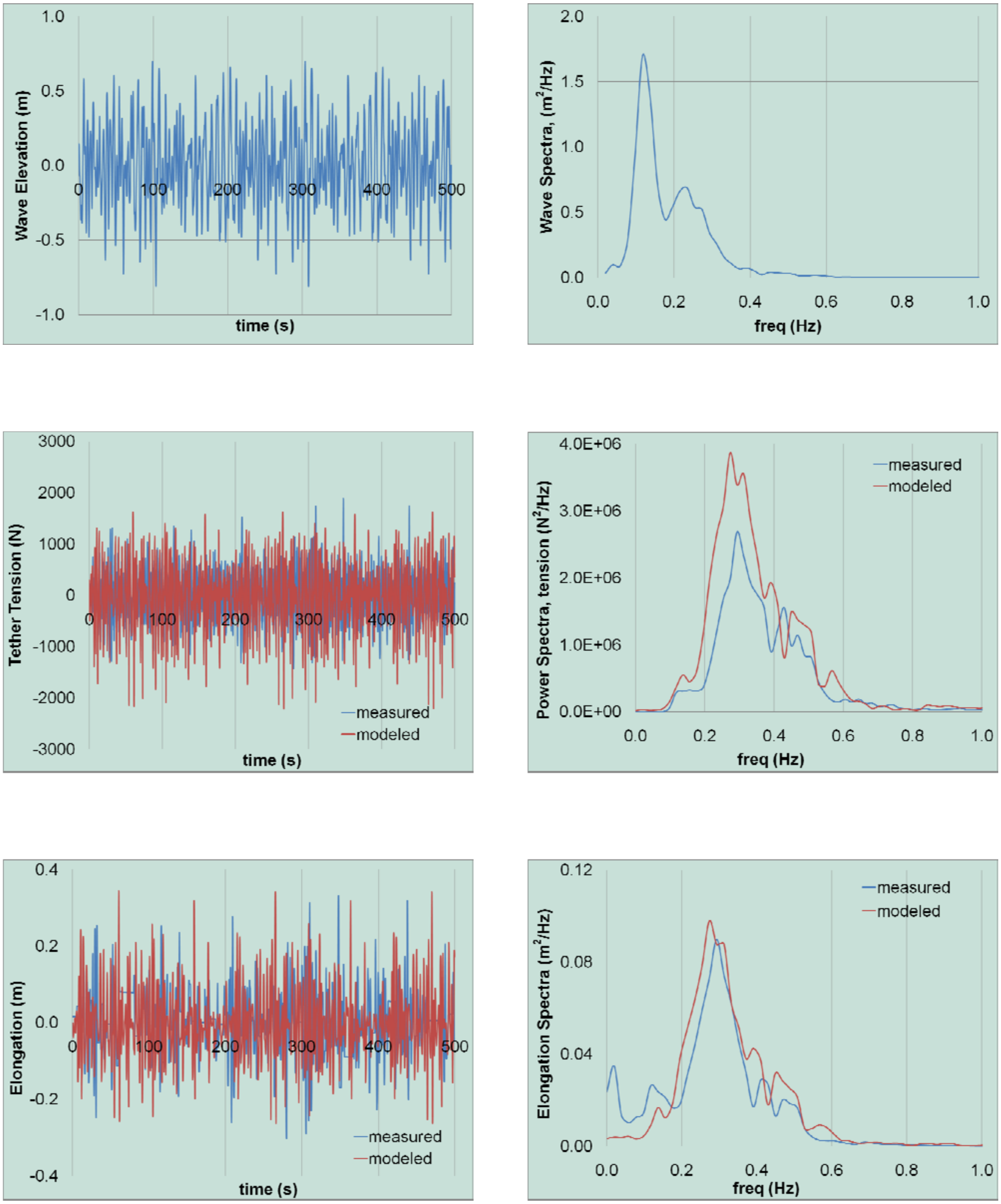

Figure 10. Time history and corresponding spectra of wave elevation, measured and modeled tether tension and elongation. (Buoy-sphere Aug 10, 2009